RSC Advances

ROYAL SOCIETY OF CHEMISTRY

www.rsc.org/advances

Journal Name

ARTICLE

Hybrid TiO_2-Acetylacetonate Amorphous Gel-Derived Material with Stably Adsorbed Superoxide Radical Active in Oxidative Degradation of Organic Pollutants

Received 00th January 20xx,
Accepted 00th January 20xx

DOI: 10.1039/x0xx00000x

www.rsc.org/

Filomena Sannino[*a,d], Pasquale Pernice[b,d], Claudio Imparato[b], Antonio Aronne[b,d], Gerardino D'Errico[c,e], Luciana Minieri[b], Marco Perfetti[c], Domenico Pirozzi[b,d]

Hybrid sol-gel TiO_2-acetylacetonate (HSGT) material has been synthesized via a sol-gel route. The as dried HSGT can be described as an amorphous polymeric network of titanium oxo-clusters on which surface part of Ti^{4+} ions are involved in strong complexation with acetylacetonate (acac) ligands. In this material a ligand-to-metal charge transfer (LMCT) is active giving light absorption in the visible region indicating a band gap of 2.5 eV, lower than crystalline TiO_2. In the HSGT gel derived material the LMCT mechanism results much more active respect to ligands on crystalline nanoparticles. In presence of air, the acac ligands on the HSGT surface are able to generate and stabilize superoxide radical as resulting by EPR measurements. The $^{\bullet}O_2^-$ radicals were stably adsorbed on the HSGT at room temperature for very long time. The presence of these free radicals makes HSGT material a useful catalyst in degradation of organic pollutants. Its catalytic activity has been tested in the oxidative degradation of phenanthrene resulting in a fast degradation rate in absence of any light irradiation.

1 Introduction

TiO_2 based materials are widely studied for their photocatalytic application in various fields, such as oxidative degradation of organic pollutants in environmental remediation, solar chemical conversion in processes as water spitting, CO_2 reduction and dye sensitized solar cell production.[1-6] However, in the semiconductor-assisted photocatalysis TiO_2 is not very efficient owing to its wide band-gap (~3.2 eV for anatase and ~3.0 eV for rutile) that allows it to absorb less than 5% of solar light radiation. Therefore, a great deal of interest has been devoted to extending the optical response of titanium oxide in the visible region that is only about 45% of solar energy. The common way to modify large band-gap semiconductors is the doping with metallic or non-metallic elements that generate intermediate energy state in the lattice.[1,2] The electronic transitions between the semiconductor bands and dopant levels occur by absorbing visible light. TiO_2 has been also activated in the visible by coupling with others semiconductors having lower band-gap.[7,8] Moreover, Co_2O_3-TiO_2 active in the degradation of pollutants both in the dark and under visible light irradiation also showed significant thermocatalytic activity.[9] More recently, TiO_2 based hybrid heterostructure nanocomposite have been synthesized resulting in more efficient utilization of the solar spectrum.[10-12] Rational design of complex heterostructures, as in the case of the core–shell YF_3:Yb,Tm@TiO_2 nanostructures not only allows an excellent photocatalytic activity under the UV irradiation but also work in the NIR band, as the core nanoparticles can efficiently upconvert NIR light into UV one, with responses to a broader spectral range.[13]

Visible light activation of TiO_2 crystalline nanoparticles as well as of other wide band-gap semiconductors can also be achieved through the surface absorption of organic molecules that occur in two different sensitization mechanisms. In the first one, relatively large dye molecules are adsorbed onto an oxide surface and electronic transition between HOMO and LUMO of dye molecules occurs by absorbing a visible light photon. Electrons are then injected from the excited dye molecule into the conduction band of the semiconductor. This first mechanism has been extensively studied in common dye-sensitized solar cells.[14-16] In the second mechanism, relatively small organic molecules adsorbed on the oxide surface form a charge transfer (CT) complex that absorbs in the visible region at energy lower than either the chelating molecules or the oxide particles. In this case, direct injection of an electron from

[a] Università di Napoli Federico II, Dipartimento di Agraria, Via Università 100, I-80055 Portici (Na), Italy.
[b] Università di Napoli Federico II, Dipartimento di Ingegneria Chimica, dei Materiali e della Produzione Industriale, P.le Tecchio 80, I-80125 Napoli, Italy.
[c] Università di Napoli Federico II, Dipartimento di Scienze Chimiche, Complesso Universitario Monte Sant'Angelo, Via Cinthia, I-80126 Napoli, Italy
[d] Centro Interdipartimentale di Ricerca sulla Risonanza Magnetica Nucleare per l'Ambiente, l'Agro-Alimentare ed i Nuovi Materiali (CERMANU), Università di Napoli Federico II, Via Università 100, I-80055 Portici (Italy)
[e] Consorzio Interuniversitario per lo Sviluppo dei Sistemi a Grande Interfase, Unità di Napoli, Complesso Universitario Monte Sant'Angelo, Via Cinthia, I-80126 Napoli, Italy.

† Footnotes relating to the title and/or authors should appear here.
Electronic Supplementary Information (ESI) available: [details of any supplementary information available should be included here]. See DOI: 10.1039/x0xx00000x

the ground state of the molecule into the conduction band of the oxide occurs without involvement of any excited molecular state. This direct charge transfer from the HOMO of the adsorbed molecule to the conduction band (CB) of the oxide, has to be seen as ligand-to-metal charge transfer (LMCT) process.[1,2] Among electron rich ligands are the oxygen-based bidentate ligands such as salicylate and salicylic, dopamine, chatecol and acetylacetone, these molecules that form a CT state with semiconductors also show surface enhanced Raman scattering (SERS) through the chemical effect.[17,18]

To achieve visible light sensitization, usually dye or small sensitizing molecules are adsorbed on previously prepared TiO_2 crystalline nanoparticles. In the present paper a hybrid TiO_2-acetylacetonate material (HSGT) has been synthesized by sol-gel route. Contrary to the usual practice, the complexing/sensitizing molecules were added directly into the solution containing the precursor of titanium obtaining a porous gel derived material with acetylacetonate molecules strongly linked on its surface giving a band-gap lowering (2.5 eV). The presence on its surface of stable free radicals made this material an active catalyst in organic pollutants degradation, with successful performance in environmental remediation processes as demonstrated using phenanthrene (PHE), a typical three-ring polycyclic aromatic hydrocarbon (PAH), as a model compound.

2 Experimental

2.1 Sol-gel synthesis

The hybrid sol-gel TiO_2 (HSGT) was prepared by a sol-gel route using titanium(IV) n-butoxide (97+%), acetylacetone (Hacac) (99+%), 1-propanol (99.80+%) and hydrochloric acid (37wt%) provided by Sigma-Aldrich. All the reagents were used without further purification. A solution containing 10 mL of titanium(IV) n-butoxide (29.1 mmol), 1.20 mL of acetylacetone (11.6 mmol) and 3.87 mL of 1-propanol (51.8 mmol) was prepared and stirred for a few minutes at 50°C. A second solution containing 5.27 mL of distilled water (291 mmol), 7.0 mL of 1-propanol (93.6 mmol) and one drop of HCl (37wt%) was then prepared and mixed with the first one. The resulting molar ratio Ti : Hacac : propanol : water was 1 : 0.4 : 5 : 10. The solution obtained was vigorously stirred at 50°C for about 5 min, until the gelation occurred. A homogeneous slightly yellow colored gel was obtained. The gel was left at room temperature for 24 h and then dried under airflow at 30 °C until constant weight, obtaining a porous amorphous material. A reference TiO_2 matrix (SGT) was also prepared in similar conditions except for the lack of acetylacetone in the solution of the Ti precursor. Consequently, when the hydro-alcoholic solution was added to the precursor solution, the instantaneous formation of a particulate gel took place.

2.2 Thermal and Structural Characterization

To study the reactions occurring during HSGT heating, thermogravimetric (TG) and differential thermal (DTA) analyses were carried out, using a TA Instruments SDT Q 600. The TG and DTA tests were performed keeping 20–25 mg of xerogel under nitrogen atmosphere, varying the temperature from 20 to 800 °C. A heating rate of 10 °C min^{-1} was adopted. The amorphous nature of the dried gels as well as the nature of the crystallising phases was ascertained by X-ray diffraction with a Philips X'PERT-PRO diffractometer by using monochromatized CuKα radiation (40 mA, 40 kV) with a step width of 0.013° 2θ. N_2 adsorption–desorption isotherms at 77 K were obtained with an Autosorb-1, Quantachrome apparatus. The sample was previously treated in the sample cell at 100 °C under vacuum up to complete degassing. The N_2 adsorption–desorption isotherms were elaborated by the Brunauer–Emmett–Teller (BET) method for the calculation of the surface areas.[19] Pore volumes were determined from the amounts of adsorbed N_2 at P/P° = 0.98 (desorption curve), assuming the presence of liquid N_2 (density = 0.807 g cm^{-3}) in the pores under these conditions. The pore size distribution was determined by application of the Barret-Joyner-Halenda (BJH) method.[19] The structure of the HSGT matrix, as well as its structural evolution during the heating, was studied by Fourier transform infrared (FTIR) spectroscopy. FTIR spectra of dried and heat-treated gel samples were carried out at room temperature by a Nicolet system, Nexus model, equipped with a DTGS KBr (deuterated triglycine sulfate with potassium bromide windows) detector. The absorption spectra were recorded in the 4000-400-cm^{-1} range with a spectral resolution of 2 cm^{-1} on samples diluted in KBr. The spectrum of each sample represents an average of 64 scans, which were corrected for the spectrum of the blank KBr.

HSGT and SGT materials have been characterized by Diffuse Reflectance UV-Vis spectroscopy (DRUV) using a Jasco spectrophotometer and $BaSO_4$ as a reference in the 200–800 nm wavelength range. The UV-Vis absorption spectra of the two materials were calculated using the Kubelka-Munk function F(R∞).

Gel-derived TiO_2 material, HSGT, has been characterized by Electron Paramagnetic Resonance (EPR). The powder samples were analyzed using an X-band (9 GHz) Bruker Elexys E-500 spectrometer (Bruker, Rheinstetten, Germany). The capillary containing the sample was placed in a standard 4 mm quartz sample tube. The temperature of the sample was regulated at 25 °C and maintained constant during the measurement by blowing thermostated nitrogen gas through a quartz Dewar. The instrumental settings were as follows: sweep width, 140 G; resolution, 1024 points; modulation frequency, 100 kHz; modulation amplitude, 1.0 G; time constant, 20.5 ms. EPR spectra were measured with attenuation of 10 dB to avoid microwave saturation of resonance absorption curve. Several scans, typically 32, were accumulated to improve the signal-to-noise ratio. The g values and the spin density of the samples were evaluated by means of an internal standard, Mn^{2+}-doped MgO, prepared by modifying a synthesis protocol reported in literature.[20] The reactants were purchased from Sigma Aldrich. MgO and $MnSO_4$ of high purity (≥ 99.99%) were used in order to prepare two aqueous solutions of $Mg(NO_3)_2$ and $Mn(NO_3)_2$, by adding nitric acid with a molar excess of 20% in respect to the metal. Proper aliquots of these solutions were mixed and a

third aqueous solution of $(NH_4)_2CO_3$ was added slowly. In order to assure a complete conversion of the nitrates into the carbonates, a large excess of $(NH_4)_2CO_3$ was employed, due to the acidic environment. The neutralization of the acidic solution was followed by the precipitation of the mixed carbonate. The precipitate was filtered and resuspended in 100 mL of distilled water in order to remove the ammonium cations, whose presence could interfere with EPR measurements. After 15 minutes, the mixed carbonate was filtered, washed twice with distilled water and dried in oven at 50°C for 24 hours. The solid was calcined at 900°C for 4 hours in a slightly reducing atmosphere (97% N_2 and 3% H_2 vol.). The Mn/Mg molar ratio in the final product was assessed to be 0.05% by ICP-MS analysis.

2.3 Catalytic Tests

Phenanthrene (99.0% purity) was purchased from Sigma-Aldrich (UK). All solvents were of HPLC grade (Carlo Erba, Italy) and were used without further purification. A stock aqueous solution of PHE 1.0 mg/L was prepared and subsequently kept refrigerated in the dark to avoid photocatalytic degradation reactions. Blanks of PHE in aqueous solution were analyzed in order to check its stability and the possible sorption to vials. The PHE removal experiments were carried out as a function of the following solid/liquid ratios R (R=mg of matrix/1 mL of PHE aqueous solution) 0.05, 0.1, 0.2, 0.4, 1.0, 2.0, 5.0 and 10 at 30°C for an incubation time of 60 min. All the tests were carried out in the dark to avoid any additional photocatalytic degradation. After incubation in a thermostatic rotary shaker at 30°C, the samples were centrifuged at 10,000 rpm for 10 min and the supernatants were analyzed by an Agilent 1200 HPLC apparatus (USA) equipped with a DAD and a ChemStation Agilent Software, as reported in detail by Sannino et al.[21] The removal (%) of PHE (X) was calculated by the following balance equation:

$$\frac{Co - C}{Co} \times 100$$

where Co and C are the concentration of PHE (mg/L) at the start and at the end of the incubation, respectively.

The PHE degradation products were extracted and identified by Gas Cromatography-Mass Spectrometry (GC-MS) analysis. In a standard experiment, 20 mL of PHE aqueous solution (1.0 mg/L) were incubated with 1.0 mg of HSGT (R=0.05) for 4h. After this reaction time, the slurry was taken out and centrifuged to remove the HSGT solid. The obtained supernatants were subjected to extraction in a separatory funnel with *n*-hexane in the ratio 1:6 (v:v). This procedure was performed three times to ensure the complete extraction of all the reaction products. Successively, the *n*-hexane layer was dried by anhydrous sodium sulphate, evaporated under reduced pressure at 30 °C, dissolved in 1 mL of dichloromethane phase and analysed by GC-MS.[21] The samples were analyzed using a Perkin-Elmer AutoSystemTM XL gas chromatograph, equipped with a Programmed-Temperature Split/Splitless injector with programmable pneumatic control kept at a constant temperature of 250 °C, a Restek Rtx-5MS capillary column (5% diphenyl-95% dimethylpolysiloxane, length 30 m, 0.25 mm ID, and 0.25 mm df), and a Perkin-Elmer TurboMass Gold mass-spectrometer.[21] The oven temperature was programmed to run at 60 °C for 5 min and then to increase by 15°C min^{-1} to a final temperature of 280 °C. Under these conditions the retention time for PHE was 12.75 min. A NIST mass spectral library version 1.7 was used for peaks identification. All the experiments were performed in triplicate and the relative standard deviation was lower than 4%.

3 Results and discussion

3.1 Sol-Gel Synthesis, Thermal and Structural Characterization of Hybrid TiO_2

Sol-gel is a well-known and very powerful technique used to synthesize solid materials both in the form of bulk or film starting from a solution. This method easily allows the preparation of an inorganic porous matrix incorporating active organic or inorganic components as oxides, metallic particles, organic molecules, enzymes and cells for many different applications: sensors, catalysis, optics etc. In the synthesis of the TiO_2-acetylacetonate hybrid material the process conditions were selected to allow obtaining a homogeneous chemical gel. Titanium alkoxides, as many of transition element alkoxides, show very high reactivity toward the hydrolysis-condensation reactions that lead quickly to a particulate gel (physical gel). Therefore when slower hydrolysis-condensation reactions are needed, as for film or bulk gel derived materials, it is necessary to control the hydrolysis reaction rate of the titanium alkoxides. β-diketones and particularly acetylacetone have been used as a complexing agent which, by stabilizing the solution, allows the gelation process. Therefore, in the present synthesis of TiO_2-acetylacetonate hybrid material, acetylacetone (*Hacac*) has a double role: i) as a complexing agent (for stabilizing the solution) and ii) reagent (i.e. constituent of the final hybrid material).

In the present case, it is important to ensure that particle aggregation is not too fast in order to allow the gelation of the solution as a whole. Due to the high stability of the titanium complexes with *acac* ligands, these *acac* ligands are expected to be still anchored to the titanium oxo-oligomeric clusters forming the wet gel, even after the hydrolysis step. By drying this wet gel, amorphous glass-like pieces of gel-derived material (xerogel), about 1 mm in size, were obtained (*Figure 1*).

The synthesized TiO_2-acetylacetonate hybrid material (HSGT) can be described as a polymeric network of titanium oxo-clusters, on the surface of which part of Ti^{4+} ions are involved in strong complexation with acetylacetonate (*acac*) ligands. In other words, even after drying, the HSGT xerogel stably holds most of the acetylacetone used in the sol-gel synthesis and can be considered an *acac* surface-modified porous TiO_2 xerogel.

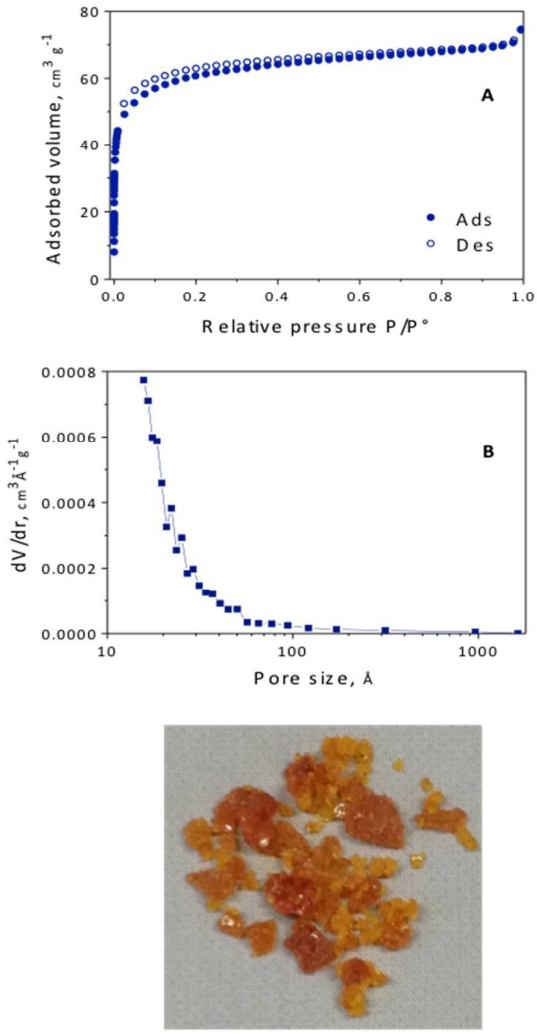

Figure 1. Hybrid TiO_2-acetylacetone xerogel dried at room temperature; A) Adsorption–desorption isotherms of HSGT, full symbols: adsorption, empty symbols: desorption; B) differential pore size distribution of HSGT.

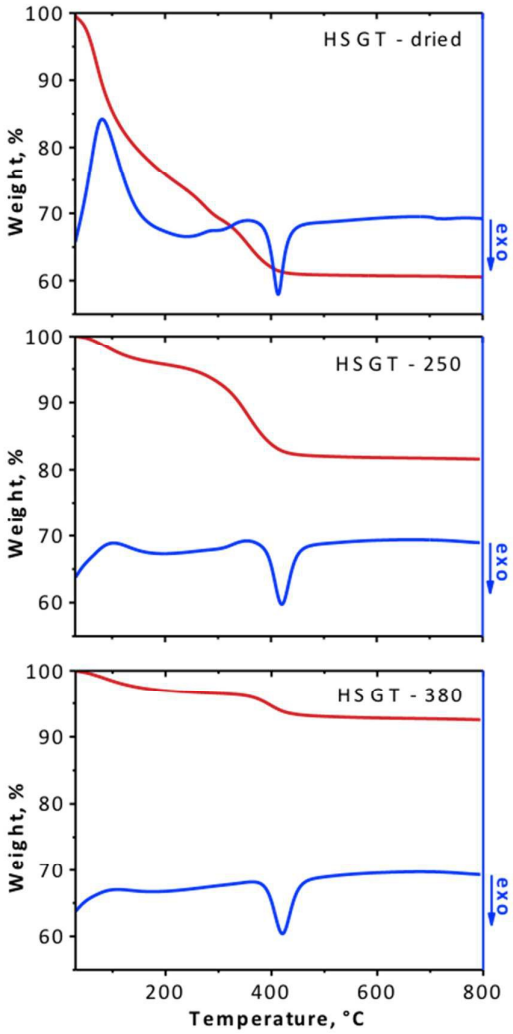

Figure 2. TG/DTA curves, recorded in nitrogen at 10 °C/ min, of HSGT as dried (HSGT-dried) and heated up to 250°C (HSGT- 250) and 380°C (HSGT-380).

The retention of the acac ligand in HSGT xerogel is indicated by the light yellow color typical of the Ti-acac complex.

The N_2 adsorption–desorption isotherms of the HSGT sample are reported in *Figure 1*. Because of the hybrid nature of the material and on the basis of the TG/DTA and FTIR results discussed below, the sample was degassed under vacuum at 100 °C allowing the evacuation of water and solvent molecules but avoiding the loss of *acac* ligands. The HSGT isotherm, of the type I according with the IUPAC classification,[22] is characteristic of a microporous material, with high amounts of N_2 adsorbed at low pressure, even if the lack of a well defined plateau at higher pressure suggests the presence of a certain amount of pores exceeding the micropore dimension. The overall surface area evaluated by the BET method was 227 $m^2 \cdot g^{-1}$. The pore size distribution evaluated by the BJH method, reported in *Figure 1*, confirms that HSGT is essentially microporous with only a small amount of pores in the mesopores size region.

To investigate the hybrid nature of the HSGT material and, in particular, to study the effect of *acac* ligands on the thermal decomposition of the xerogels, the TG/DTA analysis was employed. TG/DTA curves of fine powders HSGT xerogel, recorded in nitrogen at 10 °C min^{-1}, are reported in *Figure 2.* The TG/DTA curve of HSGT xerogel shows an overall weight loss of about 38 wt%; on the TG curve only two distinct inflection points are observed in the range 25–405 °C (~72 °C and 274 °C), the first one corresponding to a well defined DTA endothermic peak that is related to the evaporation, from open pores, of water and alcohol physically trapped in the gel. Whereas the weight loss centred at 274°C is related to the volatilization of *acac* molecules that are more strongly linked to the matrix. As seen in the following, this result is confirmed also by FTIR analysis.

The DTA curve shows an exothermic peak at about 415°C in the temperature range in which the crystallization of

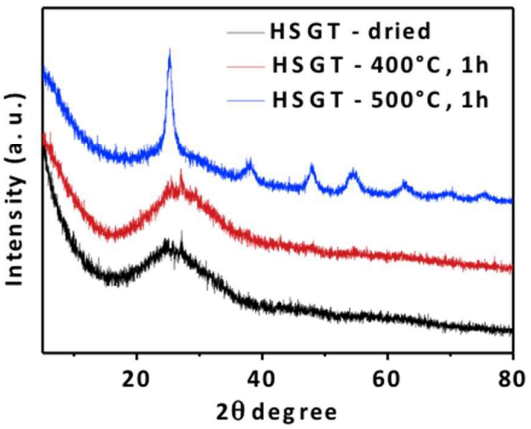

Figure 3. XRD patterns of HSGT: as-dried, heated 1h at 400°C and heated 1h at 500°C.

amorphous TiO_2 gel may occur. Indeed this exothermic peak cannot be ascribed to a crystallization process, as HSGT sample when heated at 400°C for 1 h is still amorphous: only a very small peak is seen on its XRD pattern that appears unchanged respect the initial one *(Figure 3)*. Therefore this exothermic peak must be rather attributed to a structural relaxation, a process by which excess free volume is removed, allowing the structure of the amorphous matrix to approach the configuration of the metastable liquid (glass). Because the shrinkage occurs just after the removal of the *acac* ligands, it is conceivable that in this case the excess free volume removed during structural relaxation is mainly that created the by *acac* loss. Only at the temperature of the DTA exothermic peak the network has acquired an enough low viscosity for this irreversible, exothermic skeletal densification. It may be argued that overlapped to structural relaxation process further condensation of the matrix occurs as confirmed by the additional very small weight loss. The crystallization process is very slow as demonstrated by the absence of any DTA exothermic peak at higher temperature: the consequent very slow release of the crystallization heat does not produce any evident DTA baseline deviation at 10°C min^{-1}. Only by heating 1 h at higher temperature (500°C) anatase nanocrystals are formed (*Figure 3*). It is worth noting that no further weight loss was observed at temperature above the DTA exothermic peak.

For a better understanding of the processes occurring during the HSGT heating and to identify the nature of each TG/DTA features, two different heat-treated samples were prepared, by heating at 10 °C min^{-1} up to the selected temperature and then quenching. A first HSGT sample was heated up to 250°C (the onset of the weight loss centered at the second inflection point of TG); the second sample was heated up to 380°C (the onset of the DTA exothermic peak). Hereafter these samples will be noted by the acronym HSGT followed by the heat-treatment temperature, i.e. HSGT-250, HSGT-380 respectively. The DTA curve of HSGT-250 (see *Figure 2*) still exhibits a residual and low intensity endothermic peak at low temperature (~80 °C), which is related to the loss of water adsorbed during the cooling at room temperature because of the porous nature of HSGT, whereas the DTA feature at about 357 °C as well as the DTA exothermic peak remain unchanged. In the HSGT-250 sample the overall weight loss is reduced to about 18 % of which 5% can be ascribed to the water absorbed on cooling and the remaining 13% is due to the loss of the *acac* ligand. Therefore, by heating up to 250 °C the evaporation of water and alcohol physically trapped in the gels as well as the pyrolysis of organics originated during the gelation and during the heating take place, but *acac* ligands are still retained in the most part as it cannot be ruled out a small loss of *acac*. On the contrary, HSGT-380 is an almost completely inorganic and amorphous material as testified by the very small and high temperature weight loss, and its DTA curve shows unchanged the exothermic peak indicating the structural relaxation of the amorphous state of the matrix. No DTA exothermic peak is

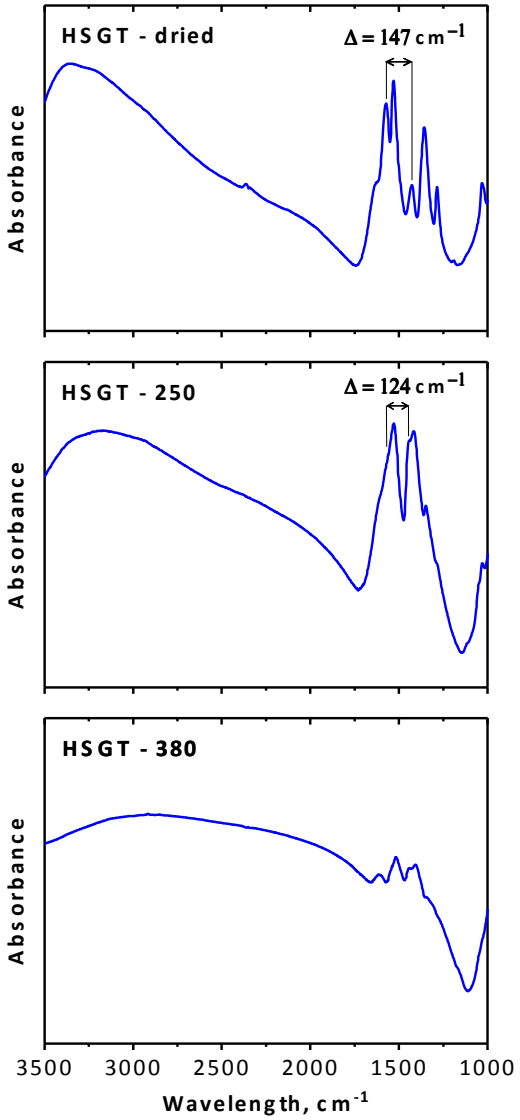

Figure 4. Room-temperature FTIR spectra of HSGT as dried (HSGT-dried) and heated up to 250 (HSGT- 250) and 380 °C (HSGT-380).

seen on the DTA curve of the HSGT previously heated 1h at 400°C (DTA curve not reported).

The hybrid nature of the HSGT can be suitably characterized also by FTIR. The spectrum shown in *Figure 4* allows affirming that in the HSGT matrix there is a bidentate interaction between the *acac* and Ti^{+4} analogously to what already seen in the case of zirconia-*acac* hybrid xerogel.[23,24] In fact, also the FTIR spectrum of the HSGT (see *Figure 4*) indicates the presence of *acac* as ligands and the splitting (Δ) between the asymmetric ($\nu_{asyC=O}$) and symmetric ($\nu_{symC=O}$) stretching of C=O bonds of the carboxylate groups, results Δ = 147 cm^{-1} lying in the 50–150 cm^{-1} range attesting the existence of a bidentate interaction between the *acac* and Ti^{4+} in the Ti-*acac* complexes.[25] Even if the spectrum of the sample HSGT-250 is a little less defined, it shows clearly that acac is still retained. On the contrary, the FTIR spectrum of HSGT-380 (see *Figure 4*) does not exhibit the characteristic absorption bands related to $\nu_{asyC=O}$ and $\nu_{symC=O}$. It shows two main absorption bands at about 1500 cm^{-1} (ν_{C-C}) and 1440 cm^{-1} (δ_{CH2}), that are related to residual organics, allowing to state the lack of Ti-*acac* complexes at this stage. This confirms further, as seen by TG data, that the *acac* ligands are almost completely retained in the sample heated up 250°C but they are completely lost in the sample heated up to 380°C.

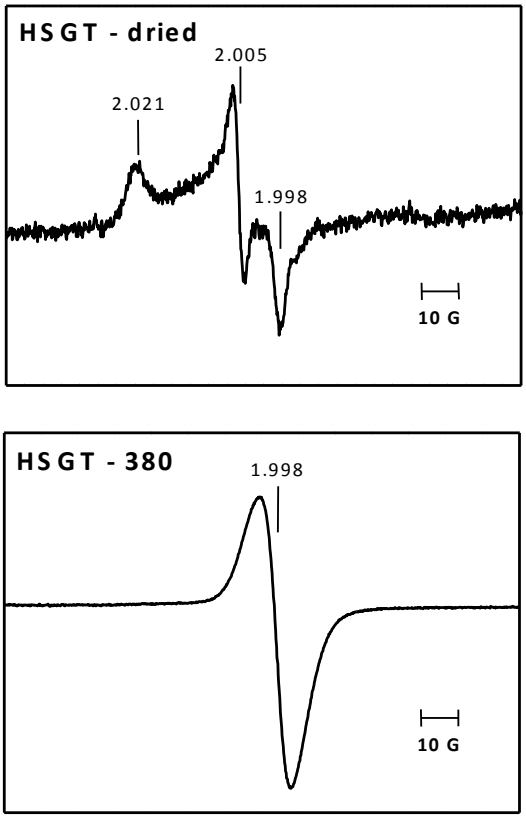

Figure 5. EPR spectra of HSGT: as-dried, heated up to380°C (HSGT-380) recorded at room temperature, g values are reported.

The high temperature value, at which *acac* is lost, indicates that *acac* ligands are strongly bonded to the solid matrix making HSGT a highly stable hybrid material. In order to reveal the presence of paramagnetic species, the hybrid gel-derived TiO_2 material (HSGT) as well as the reference titania gel without *acac* have been characterized by EPR spectroscopy. Each measurement was repeated after 12 h leaving the sample in the sample-holder of the spectrometer to avoid any light exposure. The spectrum of the HSGT powder recorded at room temperature is reported in *Figure 5* and presents a complex anisotropic lineshape that is correlated to the presence of stable radicals adsorbed on the HSGT surface. The g-tensor of this spectrum is g_{xx}=1.998 g_{yy}=2.005 g_{zz}=2.021, while the signal intensity corresponds to a concentration of paramagnetic centres of ~1.8×10^{15} spin g^{-1}. The g values are in fair agreement with values reported in the literature for the superoxide radical $^{\bullet}O_2^-$ adsorbed on solid surface of crystalline TiO_2 polymorphs,[26] small discrepancies possibly arising from the amorphous nature of our sample. Indeed the HSGT spectrum is quite similar to that reported in a previous paper for a hybrid zirconia-acetylacetone gel-derived material (HSGZ).[23] Only the g values are slightly different, therefore it can be inferred that also in the case of HSGT the EPR spectrum is due to stably adsorbed $^{\bullet}O_2^-$ species. Noticeably, the spectrum does not show any signal ascribable to Ti^{3+} ions,[27] thus excluding the presence of a significant amount of this species in the sample. Only a very weak singlet was observed for SGT (TiO_2 without acac) at a g value of about 2.00 (EPR curve not reported). This result shows that *acac* ligands play a key role in generating and stabilizing the superoxide radical anions.In the HSGT material *acac* ligands are essential to obtain $^{\bullet}O_2^-$ radical species and in their surface stabilization. In no case such radicals have been observed on oxide surface stable at room temperature. In the spectrum the sample annealed at 380°C (HSGT-380) where no *acac* is present, there is only an intense single peak at *g* = 1.998. However, no evidence of $^{\bullet}O_2^-$ superoxide anion radicals is observed, thus showing beyond any doubt that the presence of *acac* ligands is necessary to promote the $^{\bullet}O_2^-$ superoxide anion radicals formation on the material surface. $^{\bullet}O_2^-$ is a very reactive and short-live species; in solution, it can be detected only by using spin traps;[28] alternatively its role in photocatalytic degradation reaction can be indirectly studied by using suitable radical scavengers.[29-31] To our knowledge, in the literature it was never reported the formation and the stable presence of $^{\bullet}O_2^-$ radicals on TiO_2 surfaces at room temperature.

In HSGT materials, part of surface Ti^{+4} ions are complexed with *acac*, that is a redox active ligand that can exist as acetylacetonate anion $acac^-$ or as neutral radical $acac^{\bullet}$, acting as electron donor. In other words, HSGT material behaves as a charge transfer complex (CT) where a ligand-to-metal electron transfer is activated. When *acac*-to-titanium electron transfer occurs, an electron is directly injected in the 3d-Ti conduction band (CB) leaving an oxidized ligand $acac^{\bullet}$ radical. Electrons in the conduction band are able to reduce molecular oxygen O_2

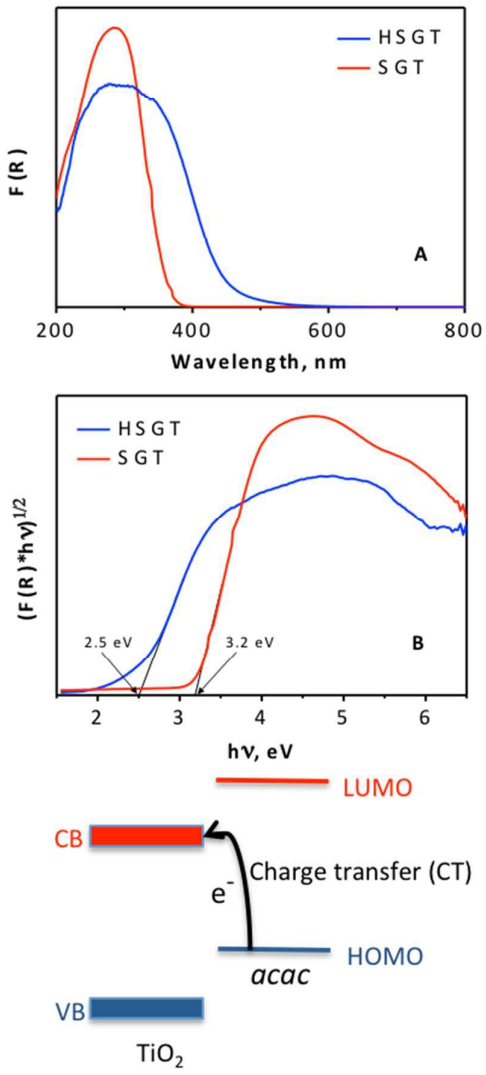

Figure 6. UV-Vis absorption spectra (A) and band gap evaluation (B) for HSGT and SGT samples.

to superoxide radical anions $^{\bullet}O_2^-$ that are then stabilized when coordinated to surface Ti^{+4} ions. We hypothesize that the ligand *acac* is fundamental not only in generating, but also in stabilizing $^{\bullet}O_2^-$ species on the HSGT surface. Recent computational studies conducted on the related hybrid zirconia-acetylacetone gel-derived material (HSGZ) have shown that the presence of complexed *acac* molecules lead to a favourable thermodynamic driving force for the adsorption of molecular oxygen species.[32] Moreover, only in the presence of the ligand the analysis of the magnetic moments on each atom of the adsorbed oxygen molecule is consistent with the formation of the superoxide radical ion.[32]

Spectroscopic techniques are able to detect chelated *acac* species that are active in CT complex as it is confirmed by DRUV measurements. The UV-Vis absorption spectra of HSGT and gel-derived titania without *acac* (SGT) materials, calculated using the Kubelka-Munk function F(R∞), are reported in *Figure 6*A. The HSGT spectrum is characterized by a broad peak centered at around 300 nm with a shoulder-like queue in the visible region up to 600 nm (*see Figure 6A*). In contrast, SGT shows an absorption edge in the UV region at wavelengths below about 390 nm. Inspection of *Figure 6A* shows that, apart from the presence of the broad peak around 300 nm, a marked red shift of the absorption edge is seen in the HSGT material with respect to SGT one.

The energy gap values were calculated by linearization of the plot of $(F(R)h\nu)^{1/2}$ against hν,[33] as reported in *Figure 6B*. For the SGT material, the evaluated optical band gap is 3.2 eV for the transition from the valence band (VB) to conduction band (CB), i.e. related to the $O^{2-} \rightarrow Ti^{+4}$ charge transfer transition. This value is in agreement with the crystalline TiO_2 literature value.[34] For the HSGT sample, a lower band gap is observed, 2.5 eV (about 500 nm).

This low value is associated to electronic transition producing the yellow-brown colour of the HSGT titania-*acac* gel material.[17] It is worth noting that the optical absorption band of HSGT in the visible range necessarily arises from the interaction between the *acac* chelating ligands and titanium ions as the two isolated components (TiO_2 and acetylacetone) adsorb light only in the UV with similar absorption edge, and free acetylacetonate ($acac^-$) has the $\pi \rightarrow \pi^*$ absorption at 272 nm.[9, 35] The extension in the visible region of the HSGT absorption clearly is indicative a mechanism of charge injection from the ligand into the conduction band of the oxide by direct excitation from the HOMO of the *acac* ligands to the 3d-(Ti) conduction band (CB).[25] This requires that the alignment of the bands at the hybrid interface is staggered as shown by the energy diagram, Figure 6. Such a CT process generates electron/hole pairs (e^-/h^+) with the holes localized on the organic ligands and the electrons in the conduction band of TiO_2. The broadness of the absorption band also indicates that there is a very broad distribution of electronic states for HSGT and all them, even those corresponding to the optical transition at the end absorption tail in the visible region, inject electrons into the conduction band.

This direct charge transfer (CT) mechanism at the interface between organic molecule-TiO_2 crystalline nanoparticles has been reported for many small molecules acting as bidentate ligands such as catechol, dopamine, salicylic acid and others.[2, 36, 37] In catechol-TiO_2 system long-term stability (minutes) of the photo-generated electron-hole radical pairs was reported[37] and related to an increased chemical reactivity of the pairs. In particular it was noted a lower charges recombination rate in nanoporous TiO_2 film with respect to the nanoparticles suspension. In nanoporous film, an extended nanocrystals network makes possible the electron delocalization resulting in an increased distance between the radical pairs with a consequent lower recombination rate.[37] In the HSGT, the extended oxide matrix can also allow electron delocalization and the consequent low recombination rate. This makes the electrons in CB highly reactive in molecular O_2 reduction to $^{\bullet}O_2^-$ superoxide radicals that are then stably linked to the HSGT surface as testified by the EPR results.

3.2 Phenantrene removal tests

The high value of hydrolytic stability makes HSGT suitable for different applications; in particular the peculiar ability of the HSGT to generate superoxide radicals in the presence of molecular oxygen makes it a useful catalyst in the oxidative degradation of water pollutants. Here the effectiveness of HSGT as a catalyst has been tested in the removal of a typical three-ring aromatic hydrocarbon phenanthrene (PHE) from aqueous solution.

Because titanium oxide is a well-known photocatalyst, the PHE removal tests were performed at 30 °C in a stirred batch system in dark condition to avoid any additional photocatalytic effect. It was used a fixed amount of HSGT (from 0.5 to 100 mg) in 10 mL of aqueous stock solution (1.0 mg/L) i.e. at solid/liquid ratio R= 0.05, 0.1, 0.2, 0.4, 1.0, 2.0 5.0 and 10, respectively. All the experiments were carried out in a 20 mL capped glass test tube. The inside air volume assured an oxygen reservoir, largely exceeding the stoichiometric amount required for the full oxidation of PHE to CO_2 and H_2O. Therefore, the tests can be considered as made at constant O_2 concentration. The results obtained showed a complete removal of the model pollutant for a value of R ranging from 0.1 to 10 after an incubation time of 60 min. The total disappearance of PHE was also recorded at R=0.1 even lowering drastically the incubation time from 60 to 10 min. These results indicate a very high removal rate, and are quite different respect to what previously demonstrated by us[16] which found no PHE removal at R=0.1 after 1 h incubation time by using hybrid sol-gel zirconia material (HSGZ); this highlights the higher catalytic efficiency of HSGT respect to HSGZ.

In this paper, extractive experiments of degradation products performed after incubation of PHE with HSGT at R=10 and R=5 for an incubation of 60 min did not allow the identification of any intermediate probably because the oxidative process led to a complete mineralization of molecule. In order to find out the degradation products, catalytic tests were conducted with a very low amount of solid (R=0.05) for an incubation time of 240 min. In this experiment a PHE removal of 90% was detected and the formation of degradative intermediates is demonstrated by the data reported in *Figure 7* that display the total ion chromatogram. According to the standard spectra in NIST 1.7 library data, the peaks at RT of 12.65, 16.47, 17.75, 19.00 and 19.79 min could be assigned to phenanthrene, heptadecanoic acid, octadecanoic acid, hexadecanoic acid and 1,2 benzenedicarboxylic acid, bis (2-methylpropyl)ester, respectively. The analysis of degradation products is in agreement with the ones previously reported in the literature[38, 39] and by us.[21] Phthalates such as bis(2-ethylhexyl)phthalate[21] and benzenedicarboxylic acid, bis (2-methylpropyl)ester are the main intermediates of phenanthrene photodegradation by TiO_2 under UV irradiation,[38, 39] in addition, residual alkanoic acids as heptadecanoic acid, octadecanoic acid and hexadecanoic acid were identified in this investigation. These findings are in complete agreement with those reported in the literature[21,38,39] so indicating the high catalytic efficiency of HSGT without any light irradiation in oxidative degradation of very stable organic pollutants.

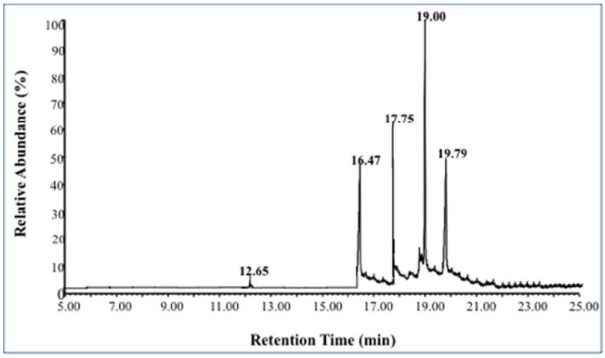

Figure 7. Total ion chromatogram of PHE catalytic degradation products after 4 h incubation time and R = 0.05.

Conclusions

The hybrid sol-gel TiO_2-acetylacetonate material (HSGT) has been synthesized by sol-gel route. Contrary to the usual practice, the complexing/sensitizing molecules were added directly to the solution containing the precursor of titanium.

The porous gel derived material produced was amorphous with acetylacetonate molecules strongly linked on its surface forming a charge transfer complex (CT) that absorbs in the visible region with a lowering of the band-gap (2.5 eV). In the presence of air, the acac ligands on the HSGT surface generate and stabilize superoxide radicals. The presence on its surface of stable free radicals ascertained by EPR made this material an active catalyst in organic pollutants degradation. The catalytic efficiency in the dark of HSGT has been demonstrated by the very fast degradation rate of phenanthrene, an organic recalcitrant pollutant.

References

1 S. G. Kumar, L. G. Devi, *J. Phys. Chem. A*, 2011, **115**, 13211-13241.
2 G. Zhang, G. Kim, W. Choi, *Energy Environ. Sci.*, 2014, **7**, 954-966.
3 W.-J. Ong, , L.-L. Tan, S.-P. Chai, S.-T. Yong, A. R. Mohamed, *ChemSusChem*, (2014), 690–719.
4 Z. Tachan, I. Hod, A. Zaban, *Adv. Energy Mater.*, 2014, **4**, 1301249.
5 X. Zhang, X. Li, Q. Zhang, J. Yang, N. Deng, *Catal. Commun.*, 2011, **16**, 7-10.
6 G. Kim, S. H. Lee, W. Choi, *Appl. Catal B: Environ.,* 2015, **162**, 463-469.
7 H. Tada, Q. Jin, A. Iwaszuk, M. Nolan, *J. Phys. Chem. C,* 2014, **118**, 12077-12086.
8 M. Pelaez, N. T. Nolan, S. C. Pillai, M. K. Seery, P. Falaras, A. G. Kontos, P. S. M. Dunlop, J. W. J. Hamilton, J. A. Byrne, K. O'Shea, M. H. Entezari, D. D. Dionysiou, *Appl. Cat. B: Environmental*, 2012, **125**, 331–349.
9 Q. Jin, H. Yamamoto, K. Yamamoto, M. Fujishima, H. Tada, *Phys. Chem. Chem. Phys.,* 2013, **15**, 20313-20319.

10 S. Bai, L. Wang, X. Chen, J. Du, Y. Xiong, *Nano Res.*, 2015, **8**, 175-183.
11 W.-J. Ong, , L.-L. Tan, S.-P. Chai, S.-T. Yong, A. R. Mohamed, *Nano Res.*, 2014, **7**, 1528-1547.
12 W.-J. Ong, , L.-L. Tan, S.-P. Chai, S.-T. Yong, A. R. Mohamed, *Nanoscale*, 2014, **6**, 1946–2008
13 Z. Li, C. Li, Y. Mei, L. Wang, G. Du, Y. Xiong, *Nanoscale*, 2013, **5**, 3030-3036.
14 T.Nakahira, M. Grätzel, *Macromol. Rapid Commun.,* 1985, 6, 341-347.
15 B. O'Regan, M. Grätzel, *Nature*, 1991,353,737-740.
16 K. Vinodgopal, D. E. Wynkoop, P. V. Kamat, *Eviron. Sci. Technol.*, 1996, 30,1660-1666.
17 D. Finkelstein-Shapiro, S. Hurst Petrosko, N. M. Dimitrijevic, D. Gosztola, K. A. Gray, T. Rajh, P. Tarakeshwar, V. Mujica, *J. Phys. Chem. Lett.,* 2013, **4**, 475−479
18 A. Musumeci, D. Gosztola, T. Schiller, N. M. Dimitrijevic, V. Mujica, D. Martin, T. Rajh, *J. Am. Chem. Soc.,* 2009, **131**, 6040–6041.
19 F. J. Rouquerol, K. Sing, Adsorption by Powders and Porous Solids: Principles, Methodology and Applications; Academic Press: London, 1999.
20 V. N. Yordanova, V. Gancheva, V. A. Pelova, *J. Radioanalyt. Nucl. Chem.,* 1999, **240**, 619-622.
21 F. Sannino, D. Pirozzi, G. Vitiello, G. D'Errico, A. Aronne, E. Fanelli, P. Pernice, *Appl. Catal. B: Environ.,* 2014, **156-157**, 101–107.
22 IUPAC Recommendations, *Pure Appl. Chem*., 1985, **57**, 603-609.
23 F. Sannino, P. Pernice, L. Minieri, G. A. Camandona, A. Aronne, D. Pirozzi, *ACS Appl. Mater. Interfaces,* 2015, **7**, 256-263.
24 A. Aronne, F. Sannino, S. R. Bonavolontà, E. Fanelli, A. Mingione, P. Pernice, *Environ. Sci. Technol.,* 2012, **46**, 1755-1763.
25 A. K. Singh, B. P. Baranwal, *Spectrochim. Acta Part A,*, 2012, **98**, 302-306.
26 E. Carter, A. F. Carley, D. M. Murphy, *J. Phys. Chem. C*, 2007, **111**, 10630-10638.
27 M. Chiesa, M. C. Paganini, S. Livraghi, E. Giamello, *Phys. Chem. Chem. Phys*., 2013, **15**, 9435-9477.
28 D. Spasiano, R. Marotta, I. Gargano, I. Di Somma, G. Vitiello, G. D'Errico, R. Andreozzi, *Chem. Eng. J.*, 2014, **249**, 130–142.
29 J. Yu, Q. Li, S. Liu, M. Jaroniec, *Chem. Eur. J.*, 2013, **19**, 2433-2441.
30 Q. Xiang, D. Lang, T. Shen, F. Liu, *Appl. Catal. B: Environ.*, 2015, **162**, 196-203.
31 Q. J. Xiang, J. G. Yu, M. Jaroniec, *J. Am. Chem. Soc.*, 2012, **134**, 6575-6578.
32 A. B. Muñoz-García, F. Sannino, G. Vitiello, D. Pirozzi, L. Minieri, A. Aronne, P. Pernice, M. Pavone, G. D'Errico, *ACS Appl. Mater. Interfaces*, 2015, **7**, 21662-21667.
33 J. Tauc, R. Grigorovici, A. Vancu, *Phys. Status Solidi*, 1966, **15**, 627-637.
34 I. A. Jankovic, Z. V. Saponjic', E. S. Dzunuzovic', J. M. Nedeljkovic', *Nanoscale Res. Lett.,* 2010, **5**, 81-88.
35 N. Petkova, S. Dlugocz, S. Gutzov, *J. Non-Cryst. Solids,* 2011, **357**, 1547-1551.
36 S. Varaganti, G. Ramakrishna, *J. Phys. Chem. C,* 2010, **114**, 13917-13925.
37 25.T. Lana-Villarreal, A. Rodes, J. M. Pérez, R. Gomez, *J. Am. Chem. Soc.,* 2005, **127**, 12601-12611.
38 Y. Zhang, J. W. C. Wong, L. Peihong, Y. Min, *J. Hazard. Mater.,* 2011, **191**, 136-143.
39 H. Jia, J. Zhao, X. Fan, K. Dilimulati, C. Wang, *Appl. Catal. B: Environ.,* 2012, **123**, 43-51.